ISSN 1063-7737, Astronomy Letters, 2009, Vol. 35, No. 4, pp. 261–269. © Pleiades Publishing, Inc., 2009.
Original Russian Text © G.N. Kichigin, 2009, published in Pis'ma v Astronomicheskiĭ Zhurnal, 2009, Vol. 35, No. 4, pp. 295–303.

On the Origin of Energetic Particles in the Foreshock Region of the Earth's Bow Shock

G. N. Kichigin*

Institute for Solar–Terrestrial Physics, Russian Academy of Sciences, Siberian Branch, P.O. Box 4026, Irkutsk, 664033 Russia

Received April 9, 2008

Abstract—We consider the processes related to the formation of the so-called foreshock region upstream of the Earth's bow shock. We suggest a model based on the surfing of pick-up ions in the bow shock front in terms of which the ion acceleration mechanism in the front can be explained. We ascertain the physical conditions under which the accelerated ions lie upstream of the shock front and determine the direction of motion of the energetic ions. We conclude that it is this population of energetic ions (longitudinal beams) that plays a major role in forming the ion foreshock boundary.

PACS numbers : 52.30.Cv; 95.30.Qd
DOI: 10.1134/S1063773709040069

Key words: *plasma astrophysics, hydrodynamics, and shock waves.*

INTRODUCTION

Using spacecraft, it has now been firmly established (Tsurutani and Rodriguez 1981; Paschmann et al. 1981; Bonifazi and Moreno 1981a, 1981b; Fuselier 1994; Eastwood et al. 2005; Oka et al. 2005) that the so-called foreshock region whose formation is attributable to the curvature of the Earth's bow shock (EBS) exists upstream of the EBS. Observations show (Tsurutani and Rodriguez 1981) that there exist two boundaries that separate the electron and ion foreshock regions from the undisturbed solar wind plasma. The foreshock picture in the plane of the ecliptic is schematically presented in Fig. 1. In this figure, the electron foreshock boundary virtually coincides with the interplanetary magnetic field (IMF) line tangential to the EBS front (point a), while the ion foreshock boundary is the (thick) line starting at point b of the EBS front. Figure 1 shows the foreshock region located on the morning side of the magnetosphere. We will restrict our analysis precisely to this foreshock region. In fact, there also exists a second foreshock region that lies in the evening sector (below point a in Fig. 1) and in which the same processes as those in the morning foreshock take place.

In this paper, we will deal with the ion foreshock region in which high-amplitude oscillations and waves are recorded and ions with energies from several keV to hundreds of keV are observed (Tsurutani and Rodriguez 1981; Paschmann et al. 1981; Bonifazi and Moreno 1981a, 1981b; Fuselier 1994; Eastwood et al. 2005; Oka et al. 2005). The foreshock ions are arbitrarily divided by the shape of their energy distribution into five groups (Oka et al. 2005): (1) beams moving along the foreshock boundary that are called either reflected ions or longitudinal beams; (2) diffuse ions; (3) intermediate ions (with signatures of the first two groups); (4) gyrating ions; and (5) ions grouped into packets with the same gyrophase. Out of these five groups, only the origin of the gyrating ions has a simple explanation — these are the ions reflected from the potential jump in the EBS front and then gyrating in the IMF. The formation mechanism of all the remaining groups of energetic ions has not yet been well established.

The origin of the ion beams moving along the boundary of the foreshock upstream of the quasi-perpendicular shock ($45° < \theta_{Bn} < 90°$, where θ_{Bn} is the angle between the normal to the EBS front and the IMF vector) arouses the greatest interest. Their properties have been studied adequately (Tsurutani and Rodriguez 1981; Paschmann et al. 1981; Bonifazi and Moreno 1981a, 1981b; Fuselier 1994; Eastwood et al. 2005; Oka et al. 2005). We will call them longitudinal beams and provide typical parameters of this population of energetic ions. They begin to move from some local region of the quasi-perpendicular EBS front and continue to move along the ion foreshock region. The location of the boundary is believed to be determined by the motion of ions along the IMF and

*E-mail: king@iszf.irk.ru

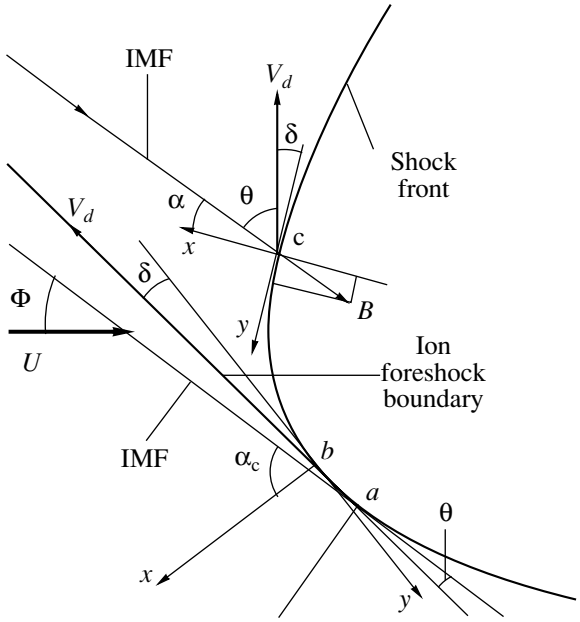

Fig. 1. Schematic view of the Earth's bow shock and the foreshock region in the plane of the ecliptic. The solar wind stream flows with a velocity U onto the shock front from the left at an angle Φ to the IMF lines. The IMF line at point a touches the shock front. The boundary that separates the foreshock region from the undisturbed solar wind plasma is indicated by the thick line emerging from point b of the shock front.

their simultaneous drift (convection) with the solar wind stream. (Below, we consider a model in terms of which a different, new interpretation of the formation of the ion foreshock boundary is offered). The measured longitudinal beam velocity varies within the range 3–5 U, where U is the solar wind velocity. The typical energy spectrum of the beam protons has a maximum near 5 keV or higher, their temperature is 100–700 eV, and the full width of the spectrum at half maximum reaches 30 keV. The number density of the longitudinal proton beams accounts for less than one percent of the proton number density in the solar wind plasma. The alpha particle number density in the longitudinal beams is lower than that in the solar wind by three or four orders of magnitude. The longitudinal beams are observed mostly in the shock front regions where the angle θ_{Bn} varies within the range $50^\circ < \theta_{Bn} < 75^\circ$, i.e., in those regions where the EBS is assumed to be quasi-perpendicular.

The existing models (Sonnerup 1969; Paschmann et al. 1980; Gosling et al. 1982; Schwartz et al. 1983) that purports to explain the origin of the longitudinal beams find no unambiguous confirmation in experiments. The most popular explanation for the origin of the longitudinal beams is given in one of the most recent reviews by Bale et al. (2005), who provided new Cluster satellite data and touched on the problem of their origin: the reflection of some of the ions from the EBS potential jump followed by their acceleration and scattering by turbulent pulsations existing in the front in such a way that some of the ions move along the foreshock boundary. The ion acceleration mechanism has not been established. In this review, attention is focused on the Cluster results, which suggest that the longitudinal beams are formed inside the EBS front, in the region of the main jump in magnetic field and density. In this paper, we propose a model based on the surfing acceleration of pick-up ions in the EBS front (Kichigin 1992, 1995; Shapiro and User 2003; Kichigin and Strokin 2007) in terms of which we show that energetic ions are generated inside the EBS front. We also ascertain the origin of the accelerated particles upstream of the EBS and establish the direction of their motion with respect to the IMF vector.

FORMULATION OF THE PROBLEM AND BASIC EQUATIONS

Let us analyze the surfing particle acceleration mechanism using the EBS as an example. In what follows, the particle motion is considered in the frame associated with the shock. The essence of the surfing is that when the solar wind ions flow onto the EBS front with an average velocity U, some of the solar wind plasma particles (due to thermal straggling) cannot overcome the potential jump existing in the EBS front and are reflected from the front. Under certain conditions, the Lorentz force acting upstream of the EBS can turn these reflected particles back toward the shock front and, in this way, the particles can be picked up by the shock for a long time and can be accelerated by the force $qUB_\perp/c$ to high energies (here, $B_\perp$ is the IMF component transverse to the direction of shock motion, q is the particle charge, and c is the speed of light). A remarkable feature of the surfing is that the same electromagnetic fields existing near the EBS front provide both particle pick-up and acceleration.

We will consider the problem of surfing ion acceleration in the EBS front. Such a problem was solved by Kichigin and Strokin (2007) through numerical calculations in the most general formulation, in which both the IMF vector and the velocity of the solar wind ion stream incident on the EBS front are assumed to be oriented arbitrarily with respect to the shock front plane. Here, we will restrict ourselves to a simpler formulation of the problem that presents a typical situation for the EBS. More specifically, we assume that the IMF vector lies in the plane of the ecliptic and that the angle between the solar wind velocity vector and the IMF vector is constant and equal to Φ. Since the width of the EBS front is immeasurably

smaller than the characteristic size and curvature of the EBS, which are comparable to the sizes of the magnetosphere, we assume the segment of the EBS front under consideration to be planar and restrict ourselves to a one-dimensional analysis. For the local planar piece of the front, we will direct the Ox axis away from the Earth perpendicularly to the EBS front (along the normal). The problem will be solved in the frame associated with the EBS.

Taking into account the adopted geometry of the EBS front, we assume the shock front in the EBS frame to be a plane layer bounded along the x axis from $x = -d$ to $x = 0$. We believe the introduction of a potential jump in the EBS front to be a fundamentally important point of our analysis, i.e., we take into account the perturbation of the potential $\varphi(x)$ in the front, which is assumed in the case under consideration to increase linearly from zero to φ_m and to remain constant further out, behind the front. It thus follows that the electric field is directed along the Ox axis, is uniform and constant, and has a magnitude $E = \varphi_m/d$ in the layer and is zero outside the layer. Since the spatial size of the potential jump in the shock front is often much smaller than the size of the magnetic field ramp (Balikhin et al. 2002), we will assume the magnetic field in and near the layer to be uniform and constant. Thus, we analyze the motion of particles in terms of a simplified shock front model. The main simplification is that the electric (E) and magnetic (B) field strengths within the potential jump characterizing the perturbation front are assumed to be coordinate-independent. For the surfing acceleration mechanism, an important parameter that includes E and B is $D = E/B$. For the EBS, $D \ll 1$.

Let us choose the coordinate system in such a way that the Oy axis is directed along the projection of the magnetic field vector onto the EBS front plane; the magnetic field vector will then have B_x and B_y components lying in the plane of the ecliptic. If we denote the angle between the vector $\mathbf{B}$ and the Ox axis by α ($\alpha \equiv \theta_{Bn}$), then $B_x = -B\cos\alpha$ and $B_y = B\sin\alpha$ (Fig. 1), where B is the magnitude of the magnetic field. As regards the electric field, in addition to the mentioned constant field E directed along the Ox axis in the shock frame, a uniform constant electric field $E_z = UB\sin\Phi/c$ perpendicular to the plane of the ecliptic also exists in the entire space.

In the specified electromagnetic fields, the following forces will act on an ion with mass m and charge q near the front in the shock frame:

$$F_x = q(E - v_z B_y/c) \text{ in front } (-d \leqslant x \leqslant 0),$$
$$\text{and } F_x = -qv_z B_y/c \text{ outside front } (x > 0, x < -d),$$
$$F_y = qv_z B_x/c,$$
$$F_z = q(UB\sin\Phi/c + v_x B_y/c - v_y B_x/c).$$

Consider two points, a and c, on the shock profile (Fig. 1). The IMF lines touch the shock front at point a, with the angle $\alpha = \pi/2$, i.e., the EBS at this point is exactly transverse. The motion of ions near the transverse EBS front when $D \ll 1$ was considered in detail previously (Kichigin 1992). In this case, the ions execute a two-dimensional motion in the $x0z$ plane. As our analysis shows, accelerating along the z axis under the field E_z, the pick-up particle oscillates along the x axis about $x = 0$, slowly drifts in the negative direction of the x axis, and, in the long run, goes behind the shock front ($x < -d$). For $D \ll 1$, the ion pick-up and, hence, acceleration ceases when the velocity component v_z approaches cD; in this case, the ion has the maximum possible energy: $E_{Km} \approx mc^2D^2/2$. Having escaped from the pick-up, the ion gyrates with the velocity cD in the downstream magnetic field while slowly receding from the front. In the literature, such particles are called gyrating ones.

As α decreases from $\alpha = \pi/2$, the limiting energy begins to increase and reaches its maximum at a certain critical angle α_c (Kichigin and Strokin 2007). As we will show below, for parameters typical of the EBS, $\beta = U/c < D \ll 1$, the critical angle α_c differs from $\pi/2$ by no more than 20°. For $\alpha_c \leqslant \alpha \leqslant \pi/2$, the accelerated ions escaped from the pick-up go behind the shock front, just as for $\alpha = \pi/2$. For $\alpha < \alpha_c$, the limiting energy decreases with decreasing α and the ions escaped from the pick-up fall into the zone upstream of the EBS (Kichigin and Strokin 2007).

Since we are interested in the dynamics of the ions that lie upstream of the shock after their acceleration, we will consider the motion of these particles at points of the EBS front for angles $\alpha < \alpha_c$. The motion of these ions in the shock frame for parameters $\beta \ll 1$ and $D \ll 1$ can be described by dimensionless equations in the nonrelativistic approximation:

$$ds/d\tau = D - v\sin\alpha, \quad (1)$$

$$dw/d\tau = -v\cos\alpha, \quad (2)$$

$$dv/d\tau = \beta\sin\Phi + s\sin\alpha + w\cos\alpha. \quad (3)$$

Here, for the velocity components normalized to the speed of light c, we use the notation $v = v_z/c$, $w = v_y/c$, $s = v_x/c$, the dimensionless time $\tau = \omega_B t$, where $\omega_B = qB/mc$, $\beta = U/c$, $D = E/B$. We will also attach an equation for the energy to the equations of motion (1)–(3):

$$d\varepsilon/d\tau = sD + \beta v\sin\Phi, \quad (4)$$

where $\varepsilon = (s^2 + w^2 + v^2)/2$ is the particle kinetic energy normalized to the ion rest mass. In Eqs. (1) and (4), $D = 0$ for $x > 0$ and $x < -d$.

The system of equations (1)–(4) is sufficient to solve the formulated problem. It can be solved analytically if it is simplified using relevant (in our case) assumptions. First, recall the necessary condition for an optimal regime of surfing acceleration — the pick-up and confinement of particles near the shock front as long as possible. The pick-up is known (Kichigin 1992, 1995) to be most optimal for particles whose velocity component v_x in the shock frame is small ($v_x \approx 0$). We will call such particles ideally picked-up ones. Note that in Shapiro and User (2003) and in other papers of these authors, the v_x velocity component of an ideally picked-up particle is assumed to increase during the acceleration. This is an erroneous assertion. In fact (Kichigin 1992, 1995), during the surfing, the acceleration of an ideally picked-up particle is peculiar in that the v_x component after the termination of the acceleration cycle is equal to its initial value, while the ($v_x \approx 0$) component during the acceleration remains small. Therefore, we will assume that the condition $s \ll \beta$ under which we can exclude the variable s from our analysis, i.e., set $s = 0$ in the zeroth approximation in Eqs. (3)–(4) and derive a system of three equations to determine three variables w, v, and ε, is met over the entire acceleration time:

$$dw/d\tau = -v\cos\alpha, \tag{5}$$

$$dv/d\tau = \beta\sin\Phi + w\cos\alpha, \tag{6}$$

$$d\varepsilon/d\tau = \beta v\sin\Phi. \tag{7}$$

RESULTS

Let us now find analytical solutions of system (5)–(7) by assuming that $\tau = \varepsilon = v_0 = w_0 = 0$ at the initial time. Taking into account the initial conditions, we will obtain solutions in the form

$$v = \rho\sin\tau_1/\cos\alpha, \tag{8}$$

$$w = -\rho(1-\cos\tau_1)/\cos\alpha, \tag{9}$$

$$\varepsilon = \rho^2(1-\cos\tau_1)/\cos^2\alpha, \tag{10}$$

where $\rho = \beta\sin\Phi$ and $\tau_1 = \tau\cos\alpha$. We obtained these solutions previously (see Kichigin and Strokin 2007). For the points on the EBS profile that lie below point a in Fig. 1, i.e., for the foreshock region lying in the evening sector of the magnetosphere, the solution will differ from (8)–(10) only in that the plus will be in front of ρ in Eq. (9) instead of the minus, i.e., the variable w will be positive.

Equations (8)–(10) are valid as long as the sign of the velocity v is positive. The point is that as soon as the sign of v becomes negative, the force F_x acting on the ion upstream of the shock changes its sign, i.e., it begins to repel the ion from the front. As a result, it will escape from the pick-up and the acceleration described by Eqs. (8)–(10) will cease. The velocity v changes its sign at the time $\tau_1 = \pi$. Solutions (8)–(10) become invalid since this time. Subsequently, receding from the front, the ion will continue its motion (drift) in the region upstream of the shock described by Eqs. (1)–(4), in which $D = 0$. These equations can also be easily solved. Measuring the time again from zero, we will assume that the velocities at $\tau = 0$ have the values $s = v = 0$ and $w = -2\rho/\cos\alpha$ obtained from (8)–(10) at $\tau_1 = \pi$. From (1)–(4) for $D = 0$, we will then obtain the solutions

$$s = \rho\sin\alpha(1-\cos\tau), \tag{11}$$

$$w = \rho\cos\alpha(1-\cos\tau) - 2\rho/\cos\alpha, \tag{12}$$

$$v = -\rho\sin\tau, \tag{13}$$

$$\varepsilon = \rho^2[2/\cos^2\alpha - (1-\cos\tau)]. \tag{14}$$

Analysis of these solutions obtained in the shock frame shows that the ion escaped from the pick-up after its acceleration drifts upstream of the EBS, with its guiding center moving in the plane of the ecliptic with the average velocity $V_\mathrm{d} = \rho(1+4\tan^2\alpha)^{1/2}$ and the velocity of its motion along the Larmor circle being ρ. It should be immediately noted that the ion gyration energy does not depend on the angle α. The ion kinetic energy related to the guiding center motion, $\varepsilon_\mathrm{d} = \rho^2(1+4\tan^2\alpha)/2$, is at a maximum at $\alpha = \alpha_\mathrm{c}$ and is $\varepsilon_m \approx 2\rho^2/\cos^2\alpha_\mathrm{c}$. Substituting the value of $\cos\alpha_\mathrm{c} \approx 0.5\pi\beta/D$ found previously (Kichigin and Strokin 2007) for $\beta/D \ll 1$, we will obtain an estimate $\varepsilon_m \approx D^2\sin^2\Phi$ for the maximum energy. For $\alpha < \alpha_\mathrm{c}$, the dependence of ε on α is described by the formula $\varepsilon = 2\rho^2/\cos^2\alpha$.

The calculated dependences of the energy on α at various values of the parameter D are presented in Fig. 2. The plots in Fig. 2 were constructed by numerically solving Eqs. (1)–(4) for the parameters indicated in this figure. The initial velocities in our calculations are $s_0 = 10^{-5}$ and $w_0 = v_0 = 0$. In this figure, the values of D are given near the curves. It follows from the shape of the curves that at a given value of D, the energy increases as the angle α decreases from $\pi/2$ to α_c, reaching its maximum at $\alpha = \alpha_\mathrm{c}$, and then decreases according to the formula $\varepsilon = 2\rho^2/\cos^2\alpha$. The calculated energies for $\alpha < \alpha_\mathrm{c}$ fall with a high accuracy (<0.1%) on the curve $\varepsilon = 2\rho^2/\cos^2\alpha$ obtained from the analytical solutions. As we see from Fig. 2, the critical angle α_c is controlled by the parameter D. Figure 3 shows the calculated dependence of the critical angle α_c on D. When $D \to 1$, $\alpha_\mathrm{c} \to \pi/2$.

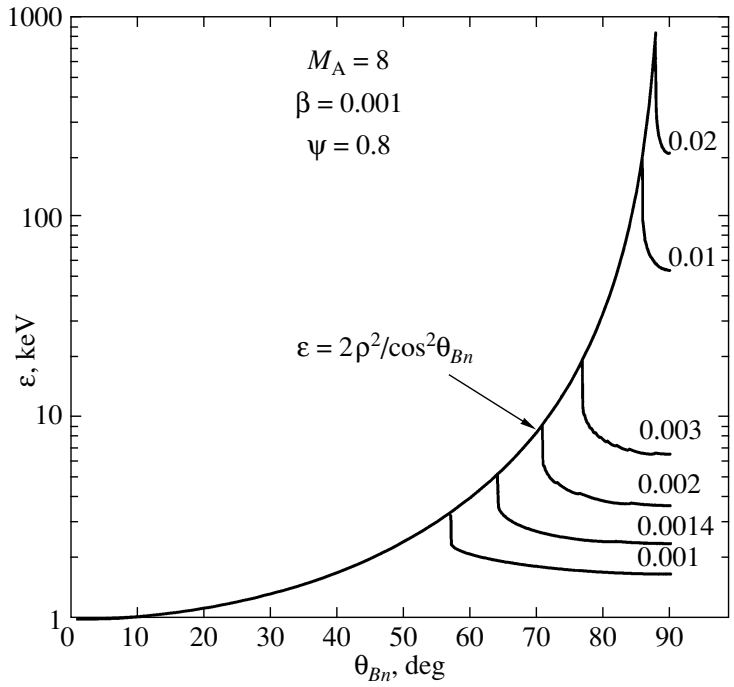

Fig. 2. Energy of surfing-accelerated ions versus angle θ_{Bn} for various values of the parameter D. For each D, the ion energy has a maximum at some critical angle $\theta_{Bn} = \alpha_c$. All of the maximum energies lie on the curve $\varepsilon = 2\rho^2/\cos^2\theta_{Bn}$.

Thus, we obtained the following patterns of motion of the ions that were initially picked up in the EBS front, were accelerated in it, and subsequently escaped into the upstream region. The acceleration of these ideally picked-up ions is described by Eqs. (5)–(7) with solutions (8)–(10). These solutions "work" until the ions escape from the pick-up. Once the ions have escaped from the front and have fallen into the upstream region, Eqs. (1)–(4) with $D = 0$ come into effect. In the upstream region, the ion dynamics is defined by solutions (11)–(14). In fact, the ion motion upstream of the shock is the drift in a constant electric field $E_z = UB\sin\Phi/c$ and a constant magnetic field B.

Let us consider the important question about the direction of motion of the accelerated protons upstream of the shock. Denote the inclination of the drift velocity vector V_d to the Oy axis in the plane of the ecliptic by δ (Fig. 1), which can be determined from the formula

$$\tan\delta = s/w = \sin\alpha\cos\alpha/(2-\cos^2\alpha). \qquad (15)$$

We see that the angle δ is a function of only the angle α. The dependence of δ on α derived from (15) is presented in Fig. 4. It follows from this dependence that $\delta = 0$ at $\alpha = 0$ and $\alpha = \pi/2$ and has a maximum $\delta_m \approx 20^\circ$ at $\alpha \approx 35^\circ$. Although the angle α in Fig. 4 formally changes from $\pi/2$ to zero, both Eq. (15) and Fig. 4 actually have a meaning only for $\alpha < \alpha_c$. Thus, to determine the angle δ, α must be measured in Fig. 4 from α_c in the direction of its decrease. If the angle between the velocity vector V_d and the IMF lines is denoted by θ, then, as we see from Fig. 1, $\theta = \pi/2 - \alpha - \delta$. The dependence of θ on α is also presented in Fig. 4, from which we see that $\theta \approx \delta$ for $\alpha > 60^\circ$. Thus, in a rough approximation, we can assume that the drift direction is almost parallel to the y axis, i.e., the protons at each point of the shock front drift in the plane of the ecliptic almost tangentially to the front (the maximum deflection from the tangent is no more than 20°). At the extreme point $\alpha = 0$, the drift velocity is zero and the accelerated proton upstream of the shock gyrates across the magnetic field, with the gyration energy being $\varepsilon = 2\rho^2$. At the other extreme point $\alpha = \alpha_c$, the protons with maximum energies move (drift) along the foreshock boundary while gyrating in the magnetic field with the velocity ρ. In the range of angles $45^\circ < \alpha < 90^\circ$, in which the EBS is quasi-perpendicular, the protons are deflected from the IMF direction by no more than 30°. Note that the motion of the energetic protons upstream of the EBS relative to point a has such a pattern that the longitudinal beams move in different directions away from point a (in Fig. 1, the longitudinal beams propagate upward in the morning sector and rightward and downward in the evening sector).

DISCUSSION AND CONCLUSIONS

We considered the dynamics of ions moving near the EBS and obtained the following picture. A small

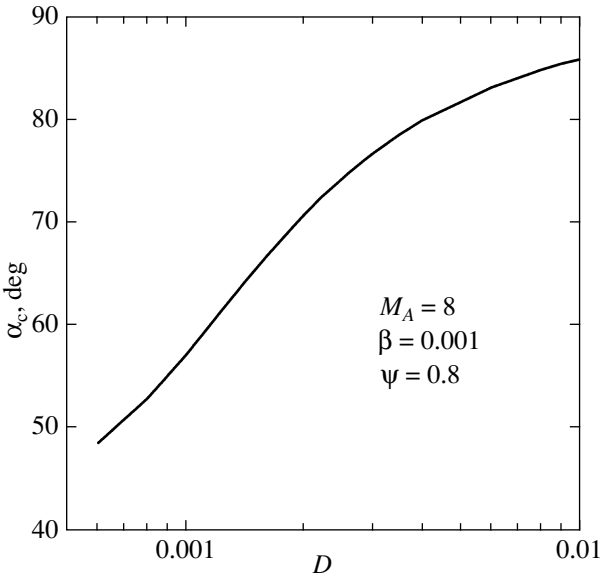

Fig. 3. Critical angle α_c versus parameter D.

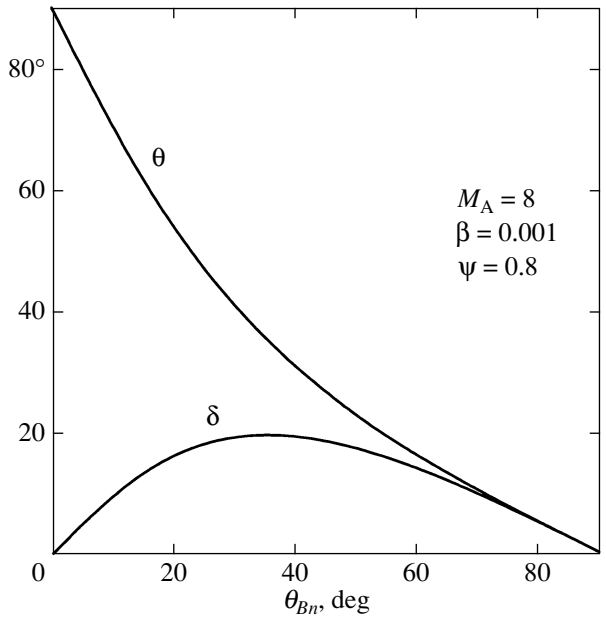

Fig. 4. Inclination of the line representing the foreshock boundary in the plane of the ecliptic (Fig. 1) to the shock front plane δ and with respect to the direction of the IMF lines (θ) versus angle θ_{Bn}.

fraction of the solar wind ions flowing onto the shock front can be picked up in the EBS front and these particles can be accelerated through surfing to high energies. The acceleration is most efficient at the points of the shock front where the angle between the normal to the front and the IMF vector is close to a right one ($\theta_{Bn} \approx \pi/2$). The pick-up ions are known (Kichigin 1992, 1995; Kichigin and Strokin 2007) to be accelerated for some finite time at $D < 1$ and, then, both their pick-up and acceleration cease. Subsequently, the behavior of the ions passed through the acceleration phase depends significantly on the angle $\alpha = \theta_{Bn}$. In the range of angles $\alpha_c \leqslant \alpha \leqslant \pi/2$, the accelerated ions fall behind the EBS front and gyrate in the magnetic field while receding from the front. In Fig. 1, these are the ions that passed through the surfing acceleration phase in the front segment a–b. Having accelerated in the front, these gyrating ions fall behind the EBS front, cross the magnetosheath, enter the Earth's magnetosphere, and, in principle, can be trapped into the radiation belts. Some of them can undergo scattering in angles in the magnetosheath by high-amplitude oscillations, which generally exist downstream of the EBS, and can fall into the morning or evening foreshock region while moving along the field lines of the magnetosheath. Below, we will consider the solar wind protons as the ions.

Some of the solar wind protons falling on the front segments where $\alpha < \alpha_c$ are picked up in the front, are accelerated, and escape into the region upstream of the EBS after their acceleration and subsequently drift there while receding from the front. These protons drift in the plane of the ecliptic. We see from the α dependence of the energy of these protons and the inclination of their trajectories with respect to the IMF vector shown in Figs. 2 and 4 that the longitudinal beams near point b have maximum energies and move at the angle δ to the EBS front plane. These protons form the forward front of the ion foreshock; as shown in Fig. 1, the inclination of the foreshock front line to the IMF lines is determined by the angle θ. As we see from Fig. 4, the angle θ between the direction of motion of the energetic particles and the IMF vector increases with decreasing angle α.

Let us discuss in detail the formation of the foreshock boundary. First of all, let us analyze what determines the inclination of the foreshock boundary to the IMF lines. First, we will present the universally accepted point of view in which the following reasoning is commonly used. The ions are accelerated in the region of the quasi-perpendicular EBS by an unknown mechanism and then some of the ions are able to move along the IMF lines and simultaneously drift with the solar wind stream from the acceleration region due to the scattering in angles. Since the longitudinal drift velocity is $V_p \approx 3$–$5\,U$, the inclination θ defined by the relation $\tan\theta = U/V_p = 1/3$–$1/5$ is $\theta \approx 11°$–$17°$. Let us now turn to the scheme of determining the geometry of the foreshock boundary suggested here. To determine the angle θ in our model, we must first know the longitudinal beam energy. Using experimental data from spacecraft measurements, let us specify this energy in the range 3–7 keV. Using

the data from Fig. 2, we will find that the critical angle for such energies is $\alpha_c \approx 60°-70°$. Finally, since, as can be seen from Fig. 4, $\delta \approx \theta$ for $\alpha_c > 60°$, we will obtain $\theta = (\pi/2 - \alpha_c)/2 \approx 12°-17°$. As we see, the values of θ in our and universally accepted models coincide. However, in contrast to the traditional point of view where only the inclination θ is explained, our model also allows the following questions about the formation of both energetic ions and foreshock to be answered in addition to the explanation of the foreshock geometry: (1) How and to what energies are the ions accelerated; (2) From which EBS region are the longitudinal beams forming the foreshock boundary injected; (3) How does the longitudinal beam energy depend on $\alpha = \theta_{Bn}$. It also explains other peculiarities noted below.

As we see from Fig. 2, the ions have a maximum energy at the critical angle α_c; the longitudinal beam energy then decreases with decreasing α as $1/\cos^2\alpha$, i.e., fairly rapidly. It is for this reason that the longitudinal beams with maximum energies are recorded in observations (Fuselier 1994) mostly in a thin layer (approximately half the Earth's radius) adjacent to the ion foreshock boundary from the inside. The critical angle α_c and the limiting longitudinal beam energy depend mainly on the parameter D, whose value, in turn, is controlled by the width of the potential jump in the EBS front, which changes from several c/ω_{pe} to several c/ω_{pi} (Balikhin et al. 2002). For the EBS under consideration, the possible values of the parameters are $\beta \approx 10^{-3}$, $D \approx 10^{-3}-10^{-1}$, and $\sin^2\Phi \approx 1/2$. For such parameters, we will obtain α_c from 85° to 60° and the limiting energies from several keV to several hundred keV. The minimum energy ε_d is reached on the shock front segments where $\alpha = 0$, i.e., in the front region where the EBS is parallel: $\varepsilon_{d\,min} = \rho^2/2$. The total energy at $\alpha = 0$ is $\varepsilon_m = 2\rho^2$, i.e., it is twice the solar wind proton energy at $\sin^2\Phi \approx 1/2$: $\varepsilon_m = 2\varepsilon_{SW}$. Typically, the solar wind proton energy ε_{SW} is of the order of or less than 1 keV. In the front region where the EBS is quasi-perpendicular ($45° < \alpha < 90°$) at $D \approx 0.1$ and $\sin^2\Phi \approx 1/2$, the proton energy will have values from tens to hundreds of keV.

In fact, the most typical energies recorded on spacecraft for the longitudinal beams lie near 5 keV (Tsurutani and Rodriguez 1981; Paschmann et al. 1981; Bonifazi and Moreno 1981a, 1981b; Fuselier 1994; Eastwood et al. 2005; Oka et al. 2005). Since the limiting energy is proportional to D^2, this means that the parameter D in the front region from which the longitudinal beams are injected is small in typical situations. Indeed, we see from Fig. 2 that $D \approx 0.0014$ at energies of 5 keV. In our case, the relation $D = E/B = 0.5M_A\psi\beta/d_P$ holds for D, where M_A is the Alfvén Mach number, $\psi = 2e\varphi_m/(mU^2)$ is the dimensionless potential jump, and d_P is the width of the EBS front in units of c/ω_{pi}. Using this relation for the parameters $\beta = 0.001$, $M_A = 8$, and $\psi = 0.8$ adopted in Fig. 2 and setting $D \sim 0.001$, we will obtain $d_p \approx 3$ for the front width. In this case, the critical angle $\alpha_c \approx 60°$ and it follows from Fig. 3 that $\delta \approx \theta \approx 15°$. The derived front width and angle θ agree well with observations. Thus, the front width in the EBS at the front points from which the longitudinal beams are injected is relatively large.

As follows from spacecraft measurements, the EBS front width at point a is at a minimum and increases as one moves along the front toward point c (Fig. 1), i.e., as the angle α decreases. This means that the parameter D will decrease with decreasing α; the local critical angle α_c, which, according to Fig. 3, is a function of D, will also decrease: $\alpha_c = \alpha_c(D)$. It may turn out that as the front width increases, i.e., as the parameter D decreases, the ions in the range of angles $\pi/2 < \alpha < \alpha_c$, i.e., on the EBS front segment $a-b$, will go behind the shock front while having an energy higher (or even much higher) than that at point b. Thus, the situation when the ions falling on the EBS front segment $a-b$ that will go behind the EBS front after their acceleration will be accelerated to energies much higher than those of the ions falling on segment $b-c$, where the longitudinal beams are generated, is quite realistic.

Let us discuss the number of ions that are involved in the surfing acceleration and that determine the longitudinal beam number density. The number of such particles is controlled mainly by the ion temperature in the plasma stream flowing onto the potential jump in the EBS front. The number of accelerated particles for a wide range of EBS parameters was calculated and given previously (Kichigin 1992). As follows from spacecraft measurements, the longitudinal proton beam number density accounts for one percent (or less) of the proton number density in the solar wind. We will obtain such a number density of accelerated protons using our previous results (Kichigin 1992) at a temperature in the front $T \approx 20-50$ eV. This is quite a reasonable value when it is considered that a fairly high level of oscillations is observed ahead of the potential jump. The ions of the solar wind onflow with a temperature of ~1 eV can be heated on these oscillations. As follows from our previous paper (Kichigin 1992), the density of the accelerated alpha particles $n_{He^{++}}$ calculated at temperatures 20–50 eV will be one and a half orders of magnitude lower than the proton density n_{H^+}. Thus, during the surfing of ions, the calculated density ratio $n_{He^{++}}/n_{H^+}$ is found to be approximately the same as that in spacecraft observations (Fuselier 1994).

The most important result of our studies is the proposed ion acceleration mechanism. It simultaneously accomplishes the ion acceleration process itself and, after the acceleration, gives the direction of ion motion upstream of the shock that determines the geometry of the foreshock boundary. Below, we present our main conclusions in detail:

(1) We pointed out the acceleration mechanism of the ions that form the population of longitudinal beams (reflected ions). The acceleration itself and the turn of the already accelerated ions in the direction of the IMF lines are accomplished through the surfing of particles in the EBS front.

(2) The inclination of the line defining the boundary that separates the solar wind plasma from the ion foreshock region to the IMF lines is approximately equal to $(\pi/2 - \alpha_c)/2$, i.e., it is determined by the critical angle α_c. This interpretation differs radically from the universally accepted one, where this inclination is believed to be related to the ion drift with the solar wind stream (Tsurutani and Rodriguez 1981; Paschmann et al. 1981; Bonifazi and Moreno 1981a, 1981b; Fuselier 1994; Eastwood et al. 2005; Oka et al. 2005).

(3) The longitudinal beams gain maximum energies at the point of the EBS front where $\theta_{Bn} = \alpha_c$. After the termination of the acceleration, the beam moves from this point upstream of the EBS at the angle $(\pi/2 - \alpha_c)/2$ to the IMF vector along the line that defines the foreshock boundary. There are no longitudinal beams at the front points where $\pi/2 > > \theta_{Bn} > \alpha_c$, in agreement with observations (Tsurutani and Rodriguez 1981; Paschmann et al. 1981; Bonifazi and Moreno 1981).

(4) For $\theta_{Bn} < \alpha_c$, the longitudinal beam energy decreases with decreasing θ_{Bn} as $1/\cos^2\theta_{Bn}$. As a result of this fact that follows from our calculations, first, the longitudinal beams with maximum energies concentrate near the EBS ion foreshock boundary (Fuselier 1994) and, second, the longitudinal beam energy decreases with decreasing θ_{Bn}. These peculiarities are confirmed by spacecraft measurements (Tsurutani and Rodriguez 1981; Paschmann et al. 1981; Bonifazi and Moreno 1981a, 1981b; Fuselier 1994; Eastwood et al. 2005; Oka et al. 2005).

(5) The inclination of the direction of the beam motion (drift) to the EBS front plane increases starting from some value at $\theta_{Bn} = \alpha_c$, reaches a maximum of 20° at $\theta_{Bn} \approx 35°$, and then decreases to zero at $\theta_{Bn} = 0$. For a quasi-perpendicular EBS, the angle between the direction of the beam drift and the IMF lines does not exceed 30°.

(6) In addition to the drift in the plane of the ecliptic, the longitudinal beams gyrate in the IMF. The energy of this gyration does not depend on the angle θ_{Bn} and is determined only by the solar wind velocity and the angle Φ between the solar wind velocity and IMF vectors. For $\sin^2\Phi \approx 1/2$ and $U \approx 300$–500 km s^{-1}, the gyration energy is ≈200–600 eV, which roughly corresponds to the observed transverse beam temperature (Tsurutani and Rodriguez 1981).

(7) The maximum longitudinal beam energies and the critical angle α_c depend mainly on the spatial width of the EBS front. As follows from our calculations, at typical beam energies of 5–10 keV observed on spacecraft, the front width is several c/ω_{pi}. In this case, the critical angle is approximately equal to 60°–70° and, hence, the inclination of the foreshock boundary line to the IMF vector is 10°–15°. These calculated values agree well with observations (Tsurutani and Rodriguez 1981; Paschmann et al. 1981; Bonifazi and Moreno 1981a, 1981b; Fuselier 1994; Eastwood et al. 2005; Oka et al. 2005).

(8) As follows from observations (Balikhin et al. 2002), the EBS front width is at a minimum (of the order of several c/ω_{pe}) at $\theta_{Bn} = \pi/2$ and then increases with decreasing θ_{Bn}. Taking this fact into account, we can assume that the ions accelerated through surfing in the range of angles $\pi/2 > \theta_{Bn} > \alpha_c$ fall behind the EBS front with energies up to several hundred keV. These ions can excite oscillations and waves downstream of the shock and can then heat the plasma through their interaction with the waves. Scattering by the oscillations existing downstream of the shock and in the magnetosheath, some of these energetic ions can fall along the field lines into the foreshock region, where they can manifest themselves in the population of the so-called diffuse ions (Tsurutani and Rodriguez 1981; Paschmann et al. 1981; Bonifazi and Moreno 1981a, 1981b; Fuselier 1994; Eastwood et al. 2005; Oka et al. 2005).

(9) The experimental fact (Fuselier 1994) of a considerably reduced (by more than an order of magnitude) ratio $n_{He^{++}}/n_{H^+}$ in the longitudinal beams compared to that in the solar wind plasma can be explained in terms of the suggested model.

REFERENCES

1. S. D. Bale, M. A. Balikhin, T. S. Horbury, et al., Space Sci. Rev. **118**, 161 (2005).
2. M. A. Balikhin, M. Nozdrachev, M. Dunlop, et al., J. Geophys. Res. **107**, 1155 (2002).
3. C. Bonifazi and G. Moreno, J. Geophys. Res. **86**, 4397 (1981a).
4. C. Bonifazi and G. Moreno, J. Geophys. Res. **86**, 4405 (1981b).
5. J. P. Eastwood, E. A. Lucek, C. Mazelle, et al., Space Sci. Rev. **118**, 41 (2005).

6. S. A. Fuselier, *Theory and Observation. Solar Wind Sources of Magnetospheric UltraLow-Frequency Waves,* Ed. by M. J. Engebretson, K. Takahashi, and M. Scholer, Geophysical Monograph 81 (Amer. Geophys. Union, Washington, D.C, 1994), p. 107.
7. J. T. Gosling, M. F. Thomsen, C. Bame, et al., Geophys. Res. Lett. **9**, 1333 (1982).
8. G. N. Kichigin, Zh. Eksp. Teor. Fiz. **101**, 1487 (1992) [Sov. Phys. JETP **74**, 793 (1992)].
9. G. N. Kichigin, Zh. Eksp. Teor. Fiz. **108**, 1342 (1995) [JETP **81**, 736 (1995)].
10. G. N. Kichigin and N. A. Strokin, Geomagn. Aéron. **47**, 745 (2007) [Geomagn. Aeron. **47**, 704 (2007)].
11. M. Oka, T. Terasawa, Y. Saito, et al., J. Geophys. Res. **110**, A05101 (2005).
12. G. Paschmann, I. Sckopke, J. Papamastorakis, et al., J. Geophys. Res. **85**, 4689 (1980).
13. G. Paschmann, I. Sckopke, J. Papamastorakis, et al., J. Geophys. Res. **86**, 4355 (1981).
14. S. J. Schwartz, M. F. Thomsen, and J. T. Gosling, J. Geophys. Res. **88**, 2039 (1983).
15. V. D. Shapiro and D. User, Planetary Sp. Sci. **51**, 665 (2003).
16. B. U. Sonnerup, J. Geophys. Res. **74**, 1301 (1969).
17. B. Tsurutani and P. Rodriguez, J. Geophys. Res. **86**, 4319 (1981).

Translated by V. Astakhov